Second-Harmonic Generation Materials

DOI: 10.1002/anie.201412344

A Facile Synthetic Route to a New SHG Material with Two Types of Parallel π-Conjugated Planar Triangular Units**

*Jun-Ling Song, Chun-Li Hu, Xiang Xu, Fang Kong, and Jiang-Gao Mao**

Abstract: *A new SHG material, namely, $Pb_2(BO_3)(NO_3)$, which contains parallel π-conjugated nitrate and borate anions, was obtained through a facile hydrothermal reaction by using $Pb(NO_3)_2$ and $Mg(BO_2)_2{\cdot}H_2O$ as starting materials. Its structure contains honeycomb $[Pb_2(BO_3)]_\infty$ layers with noncoordination $[NO_3]^-$ anions located at the interlayer space. $Pb_2(BO_3)(NO_3)$ shows a remarkable strong SHG response of approximately 9.0 times that of potassium dihydrogen phosphate (KDP) and the material is also phase-matchable. The large SHG coefficient of $Pb_2(BO_3)(NO_3)$ arises from the synergistic effect of the stereoactive lone pairs on Pb^{2+} cations and parallel alignment of π-conjugated BO_3 and NO_3 units. Based on its unique properties, $Pb_2(BO_3)(NO_3)$ may have great potential as a high performance NLO material in photonic applications.*

The exploitation of high-performance nonlinear optical (NLO) materials has attracted extensive commercial and academic interest due to their important applications in laser and photonic technologies. Typically, metal borates NLO materials, particularly for deep-UV applications, have been the focus of intensive investigations.[1–7] Currently, many efforts have been made to design noncentrosymmetric (NCS) materials by introducing NLO-active units such as π-conjugated planar units as in borates, nitrates or carbonates cations susceptible to second-order Jahn–Teller (SOJT) distortions, including cations with stereochemically active lone pairs and d^0 transition metal cations with an octahedral coordination geometry.[4–11] The combination of the above-mentioned NLO active units into a same compound can produce materials with excellent second-harmonic generation (SHG) properties.[4–11] β-BaB_2O_4 (BBO) with large π-conjugated planar $[B_3O_6]^{3-}$ units shows strong SHG response of about six times that of KH_2PO_4 (KDP).[6] The combination of borates and lone-pair-containing cations led to the discovery of $Cd_4BiO(BO_3)_3$ and $Pb_2B_5O_9I$ with larger SHG responses about 6.0 and 13.5 times that of KDP, respectively.[8,9]

[*] Dr. J.-L. Song, Dr. C.-L. Hu, Dr. X. Xu, Dr. F. Kong, Prof. J.-G. Mao
State Key Laboratory of Structural Chemistry
Fujian Institute of Research on the Structure of Matter
Chinese Academy of Sciences
Fuzhou 350002 (P. R. China)
E-mail: mjg@fjirsm.ac.cn
Homepage: http://mjg.fjirsm.ac.cn/

[**] We thank the National Natural Science Foundation of China (grant numbers 2123006, 21403232, 2137222 , and 21203197) for financial support. SHG = second-harmonic generation.

Supporting information for this article is available on the WWW under http://dx.doi.org/10.1002/anie.201412344.

$[CO_3]^{2-}$ and $[NO_3]^-$ anions which are isoelectronic with the $[BO_3]^{3-}$ unit can also be used as building blocks to design good NLO materials.

$Bi_2O_2[NO_3(OH)]$[12] and $CsPbCO_3F$[10b] with large SHG signal (≈ 6 and 13 times that of KDP, respectively) have been reported. Although these compounds possess good SHG properties, there are some inherent disadvantages, for example, poor crystallization, hydrophilicity, and relatively narrow transparency region. Additionally, their syntheses require very high reaction temperatures and very long reaction time. To date, the preparation of novel NLO borate materials with high NLO performance through a facile method remains a great challenge.

It is now well-known that increasing the density of the planar π-conjugated groups and aligning of these NLO-active units in the structures could improve the NLO performance of materials.[4,7,10,13,14] However, planar triangular BO_3 and tetrahedral BO_4 tend to be polymerized into various polynuclear clusters through corner-sharing or edge-sharing. Simple $B(OH)_3$ and $[B(OH)_4]^-$ species are almost exclusively found at the condition of appropriate pH value and boron concentration in the solution.[15,16] Recently, we have successfully prepared a series of lead-borates with different polyborate species by only adjusting the pH value of the reaction system. Besides, the introduction of triangular $[NO_3]^-$ unit into the system causes $Pb_3B_3O_7(NO_3)$ to become more structurally divers.[17] To the best of our knowledge, however, compounds containing borate and nitrate groups are still rare.[16b,18,19] All six borate-nitrate compounds reported previously contain polyborate anions such as $[B_3O_7]^{5-}$, $[B_5O_9]^{3-}$, and $[B_6O_{10}]^{2-}$ as fundamental building blocks (FBBs), hence, their BO_3 and NO_3 groups cannot be parallel to each other, rendering these materials structurally centrosymmetric and hence not SHG active. It is expected that a material composed of purely $[BO_3]^{3-}$ and $[NO_3]^-$ units that are properly aligned could exhibit large SHG coefficient due to the synergistic polarizations from these SHG active groups. Herein, we report the first polar lead nitrate-borate, namely, $Pb_2(BO_3)(NO_3)$ (LBNO), a phase-matchable material with a very large SHG response of ca. 9.0 × KDP, prepared by a facile hydrothermal synthetic route.

Single crystals of LBNO were obtained by using $Pb(NO_3)_2$ and $Mg(BO_2)_2{\cdot}H_2O$ as starting materials under only mild hydrothermal conditions.[20] Its purity was confirmed by powder XRD diffraction studies (Figure S1). The LBNO is nonhygroscopic and stable in the air at room temperature. LBNO crystallizes in the polar space group $P6_3mc$. It exhibits a two-dimensional honeycomb structure consisting of trigonal pyramids of PbO_3 and triangular BO_3 units with the NO_3 anions residing in the interlayer space (Figure 1 a). Both Pb(1)

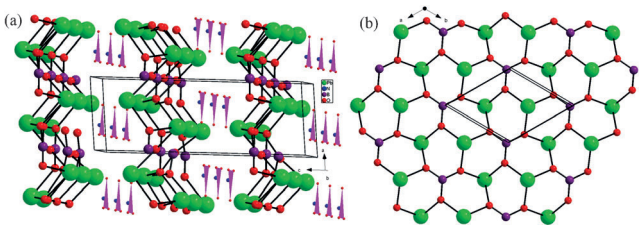

Figure 1. Crystal structure of LBNO viewed down the *b* axis (a) and a lead(II) borate layer parallel to *ab* plane (b).

and Pb(2) lying on a site of 3m symmetry are bonded to three oxygen atoms with Pb–O distances in the range of 2.31(3) to 2.34(2) Å in a trigonal pyramidal geometry,[21–26] hence both $Pb(1)^{2+}$ and $Pb(2)^{2+}$ ions show stereochemically active lone pairs. The B atom occupies a site of 3m symmetry position, it is three-coordinated in a planar triangular fashion with B–O distances of 1.39(2) Å. Each BO_3 triangle connects with six lead(II) atoms, forming a 2D $[Pb_2(BO_3)]_\infty$ honeycomb layer parallel to the (001) plane (Figure 1 b). The NO_3^- anions with N–O distances of 1.22(2) Å remain noncoordinated. They are located at the interlayer space between neighboring $[Pb_2(BO_3)]_\infty$ honeycomb layers (Figure 1 a). Furthermore, the NO_3 groups are parallel to the BO_3 groups in the $[Pb_2(BO_3)]_\infty$ layer with the dihedral angle of about 0° between $B(1)O_3$ and $N(1)O_3$, thus, all of the π-conjugated planar triangular units in the structure are arranged in a perfect parallel fashion (Figure S2).

The $[Pb_2(BO_3)]_\infty$ honeycomb layer in $Pb_2(BO_3)(NO_3)$ is somehow similar to the $[Be_2BO_3F_2]_\infty$ layer in $KBe_2BO_3F_2$ (KBBF). Three terminal oxygen atoms of the BO_3 group are linked with Pb atoms, and the elimination of dangling bonds in BO_3 triangles could be beneficial to broadening its transparence.[4] Moreover, the excellent NLO performances of the KBBF family mainly arise from the coplanar configuration of BO_3 building blocks, which promotes the large SHG response and birefringence in borates.[4,6,10] Thus, the parallel arrangement of $B(1)O_3$ and $N(1)O_3$ triangles in this compound could be favorable for its SHG performance.

The optical properties of LBNO were examined at room temperature. The result of optical diffuse reflectance spectroscopy indicates that LBNO is a wide-band-gap semiconductor with an optical band gap of 3.65 eV (Figure S3). UV/Vis-NIR absorption spectrum indicates that LBNO shows a strong absorption in the region of 200 to 334 nm mainly due to the existence of the Pb–O bonds. Hence, LBNO is almost optically transparent in the range of 0.34–2.50 μm (Figure S4). The strong IR absorption peaks observed at around 1380 cm^{-1} and in the frequency range of 1350–500 cm^{-1} confirmed the existence of NO_3 and BO_3 groups,[17,24–26] which is in agreement with the results obtained from the single-crystal X-ray structural analysis (Figure S5). LBNO is thermally stable up to about 480 °C based on TGA curves (Figure S6); the DSC diagram of LBNO exhibits two endothermic peaks at 508 and 539 °C, hence the compound melts incongruently. SHG measurements on a 1064 nm Q-switch laser with the sieved powder samples (150–210 μm)

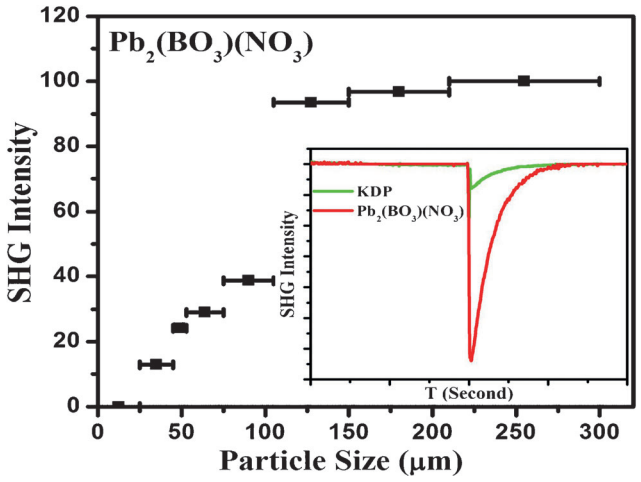

Figure 2. The phase-matching curve and oscilloscope traces of the SHG signals for the LBNO powders (inset).

reveal that LBNO exhibits a very large SHG response of ca. 9.0 times that of KDP. The plots of particle size versus SHG efficiency indicate that LBNO is also phase-matchable (Figure 2). Compared with lead nitrates or borates reported previously, such as $Pb_{16}(OH)_{16}(NO_3)_{16}$[26] and $Pb_4O(BO_3)_2$,[24b] with good alignment of BO_3 or nitrate groups showing SHG responses of about 3.5 and 3.0 times that of KDP, respectively, the NLO susceptibility of LBNO has been dramatically increased due to the arrangements of its π-conjugated BO_3 and NO_3 triangular units in a perfect parallel fashion. The polarizations of the PbO_3, BO_3, and NO_3 groups in LBNO are all directed toward the *c*-axis, their synergistic effect produces a very large SHG response for the material under laser radiation.

To better understand the optical properties and the contribution of the different NLO active groups in LBNO, theoretical calculations based on DFT methods were performed. The band structure calculations indicate that LBNO is an indirect band-gap compound (Figure S7a, from G to M). The partial densities of states (PDOS) are presented in Figure S7b. Since the linear-optical and NLO properties of materials are mainly determined by the states close to the Fermi energy, we only focus on the upper region of the valence band (VB) and the conduction band (CB) (about −10–8 eV). For clarity, the PDOS graph can be divided into VB 1–4 and CB 1–3 energy regions. It is clear that the O(1)-2s2p and N-2p states overlap fully in VB-4, and the O(2)-2p and B-2p states fully overlap in VB-3, indicating the strong N-O(1) and B-O(2) covalent interactions. Pb-6s6p and O(2)-2p are widely dispersed from VB-2 to VB-3, showing the Pb-6s6p and O(2) bonding interactions, whereas O(1)-2p nonbonding states extend over VB-1 and VB-2. In CB, the CB-1, CB-2, and CB-3 are dominated by N-O(1), Pb-O(2), and B-O(2) electronic states, respectively. Both VB maximum and CB minimum are from the electronic states of NO_3, thus, it is the NO_3 group that determines the band gap of the compound. These electronic states distribution characteristics can also be clearly observed and further verified from the orbital graphs (Figure S8,9).

The linear optical results show that the refractive indices dispersion curves display strong anisotropy and follow the order of $n^o > n^e$, indicating that LBNO is a uniaxial negative crystal (Figure S10a). The birefringence Δn is relatively large (0.174 at 1064 nm), which is favorable for the phase-matching in SHG process.

Based on the space group and the Kleinman symmetry, LBNO has two independent SHG tensors (d_{32} and d_{33}; Figure S10b). At the wavelength of 1064 nm (1.165 eV), the d_{32} and d_{33} are 1.25×10^{-8} and 5.39×10^{-9} esu, respectively. The highest tensor d_{32} corresponds to about $11.4 \times$ KDP ($d_{36} = 1.1 \times 10^{-9}$ esu), slightly higher than our measured value.

To investigate the SHG effect origin of LBNO, we calculated the SHG density of d_{32} in VB and CB (Figure 3 a,b), which is based on the band-resolved analysis and

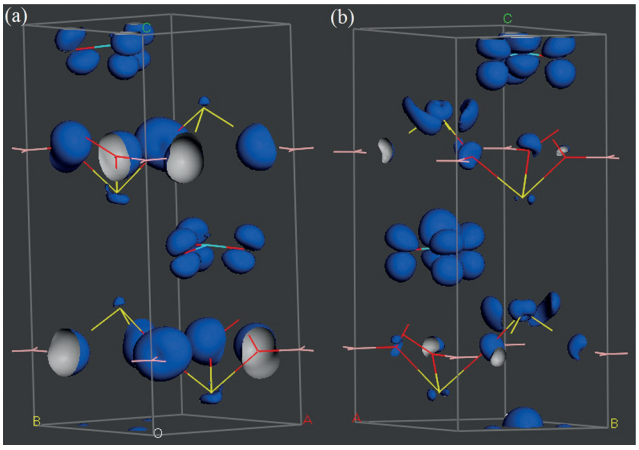

Figure 3. The SHG density of d_{32} for LBNO (a: VB, b: CB).

can intuitively give the dominant contributing orbitals to the SHG process. As shown in Figure 3, the SHG density in VB is concentrated on O atoms, specifically, some nonbonding orbitals in O(1) and O(2); and the SHG density shape is similar to the O-2p orbital graph in VB-2. The main SHG density in CB locates at the π-conjugated NO_3 group, and some at Pb(1) and O(2) atoms; and the shape in CB is very similar to the orbital graphs of CB-1 and CB-2. Therefore, the orbitals in VB-2, CB-1, and CB-2 make a significant contribution to the SHG response. Furthermore, we also carry out the integral calculations for the SHG density over VB and CB, to define the percentage of contribution to d_{32} for different NLO active units. The results show that the percentages of the contributions from the BO_3, $Pb(1)O_3$, $Pb(2)O_3$, and NO_3 units to d_{32} are 12.99%, 23.62%, 17.79%, and 41.16%, respectively, which are consistent with our discussion in the structure part, thus, the synergistic effect of the stereoactive lone-pairs on Pb^{2+} cations, two types of triangular planar BO_3 and NO_3 units resulted in a very large SHG response.

In summary, the first polar mixed anion compound with parallel BO_3 and NO_3 groups, namely, $Pb_2(BO_3)(NO_3)$, has been obtained through a facile hydrothermal synthetic route. The synergistic effect of the stereoactive lone pairs of the lead(II) cation, the π-conjugated BO_3 and NO_3 planar triangular units resulted in a very large SHG response ($\approx 9.0 \times$ KDP). Furthermore, the material is phase-matchable. It should be noted that the NLO performance of the lead(II) borate has been significantly improved due to the introduction of the nitrate groups. This study provides a new alternative approach to design and synthesize new high-performance NLO materials. We believe that this strategy could also be applied to other mixed anion systems, such as nitrate-carbonates and borate-carbonates. Our future research efforts will be devoted to the explorations of new SHG materials based on other mixed π-conjugated systems such as nitrate-carbonates and borate-carbonates.

Experimental Section

$Pb(NO_3)_2$ and $Mg(BO_2)_2{\cdot}H_2O$ were received analytically pure from Shanghai Reagent Factory (AR, 99.0%) and used without further purification. $Pb(NO_3)_2$ (0.498 g) and $Mg(BO_2)_2{\cdot}H_2O$ (0.176 g) were mixed in H_2O (12.0 mL) and sealed in an autoclave equipped with a Teflon liner (20 mL) and heated at 210 °C for 4 days. The initial and final pH values are 5.5 and 5.0, respectively. The colorless lamellar-shaped $Pb_2(BO_3)(NO_3)$ crystals were obtained in a yield of ca. 85% based on Pb. The experimental X-ray powder diffraction pattern is in agreement with the one simulated from the single-crystal crystallographic data (Figure S1). IR data (KBr cm^{-1}): 1749 (w), 1639 (w), 1389 (s), 1337 (s), 1195 (s), 1163 (s), 819 (w), 748 (m), 736 (m), 703 (m), 600 (m), 567 (m), 412 (w).

Received: December 23, 2014
Published online: February 4, 2015

Keywords: hydrothermal synthesis · lone-pair cations · second-harmonic generation · density functional calculations

[1] K. M. Ok, E. O. Chi, P. S. Halasyamani, *Chem. Soc. Rev.* **2006**, *35*, 710–717.
[2] S. V. Krivovichev, O. Mentré, O. I. Siidra, M. Colmont, S. K. Filatov, *Chem. Rev.* **2013**, *113*, 6459–6535.
[3] R. Mu, Q. Fu, L. Jin, L. Yu, G. Fang, D. Tan, X. Bao, *Angew. Chem. Int. Ed.* **2012**, *51*, 4856–4859; *Angew. Chem.* **2012**, *124*, 4940–4943.
[4] a) H. Wu, S. L. Pan, K. R. Poeppelmeier, J. M. Rondinelli, *J. Am. Chem. Soc.* **2013**, *135*, 4215–4218; b) H. W. Yu, H. P. Wu, S. L. Pan, Z. H. Yang, X. L. Hou, X. Su, Q. Jing, K. R. Poeppelmeier, J. M. Rondinelli, *J. Am. Chem. Soc.* **2014**, *136*, 1264–1267.
[5] H. Huang, J. Yao, Z. Lin, X. Wang, R. He, W. Yao, N. Zhai, C. Chen, *Angew. Chem. Int. Ed.* **2011**, *50*, 9141–9144; *Angew. Chem.* **2011**, *123*, 9307–9310.
[6] a) C. T. Chen, Y. B. Wang, B. C. Wu, K. C. Wu, W. L. Zeng, L. H. Yu, *Nature* **1995**, *373*, 322–324; b) C. T. Chen, G. Z. Liu, *Annu. Rev. Mater. Sci.* **1986**, *16*, 203–243.
[7] C. T. Chen, Y. C. Wu, A. D. Jiang, B. C. Wu, G. M. You, R. K. Li, S. J. Lin, *J. Opt. Soc. Am. B* **1989**, *6*, 616–621.
[8] W. L. Zhang, W. D. Cheng, H. Zhang, L. Geng, C. S. Lin, Z. Z. He, *J. Am. Chem. Soc.* **2010**, *132*, 1508–1509.
[9] Y. Z. Huang, L. M. Wu, X. T. Wu, L. H. Li, L. Chen, Y. F. Zhang, *J. Am. Chem. Soc.* **2010**, *132*, 12788–12789.
[10] a) S.-C. Wang, N. Ye, *J. Am. Chem. Soc.* **2011**, *133*, 11458–11461; b) G.-H. Zou, L. Huang, N. Ye, C. S. Lin, W.-D. Cheng, H. Huang, *J. Am. Chem. Soc.* **2013**, *135*, 18560–18566.
[11] W. J. Yao, H. W. Huang, J. Y. Yao, T. Xu, X. X. Jiang, Z. S. Lin, C. T. Chen, *Inorg. Chem.* **2013**, *52*, 6136–6141.

[12] R. H. Cong, T. Yang, F. H. Liao, Y. X. Wang, Z. S. Lin, J. H. Lin, *Mater. Res. Bull.* **2012**, *47*, 2573 – 2578.
[13] a) C. D. McMillen, J. W. Kolis, *Inorg. Chem.* **2011**, *50*, 6809 – 6813; b) H. S. Ra, K. M. Ok, P. S. Halasyamani, *J. Am. Chem. Soc.* **2003**, *125*, 7764 – 7765; c) H. Y. Chang, S. H. Kim, K. M. Ok, P. S. Halasyamani, *J. Am. Chem. Soc.* **2009**, *131*, 6865 – 6873.
[14] a) J. Zhao, R. K. Li, *Inorg. Chem.* **2012**, *51*, 4568 – 4571; b) R. K. Li, P. Chen, *Inorg. Chem.* **2010**, *49*, 1561 – 1565.
[15] D. Stetten Jr, *Anal. Chem.* **1951**, *23*, 1177 – 1179.
[16] S. Wang, E. M. Villa, J. Diwu, E. V. Alekseev, W. Depmeier, T. E. Albrecht-Schmitt, *Inorg. Chem.* **2011**, *50*, 2527 – 2533.
[17] J.-L. Song, C.-L. Hu, X. Xu, F. Kong, J.-G. Mao, *Inorg. Chem.* **2013**, *52*, 8979 – 8986.
[18] a) L. Y. Li, X. L. Jin, G. B. Li, Y. X. Wang, F. H. Liao, G. Q. Yao,, J. H. Lin, *Chem. Mater.* **2003**, *15*, 2253 – 2260; b) S. Wang, E. V. Alekseev, W. Depmeier, T. E. Albrecht-Schmitt, *Chem. Commun.* **2010**, *46*, 3955 – 3957; c) B.-C. Zhao, W. Sun, W.-J. Ren, Y.-X. Huang, Z. Li, Y. Pan, J.-X. Mi, *J. Solid State Chem.* **2013**, *206*, 91 – 98.
[19] a) T. S. Ortner, K. Wurst, L. Perfler, M. Tribus, H. Huppertz, *J. Solid State Chem.* **2015**, *221*, 66 – 72; b) O. V. Yakubovich, I. V. Perevoznikova, O. V. Dimitrova, V. S. Urusov, *Dokl. Phys.* **2002**, *47*, 791 – 797.
[20] Crystal data of $Pb_2(BO_3)(NO_3)$, Mr = 535.20, hexagonal, space group $P6_3mc$, $a = b = 5.0731(7)$ Å, $c = 13.040(3)$ Å, $\alpha = \beta = 90°$, $\gamma = 120°$, $V = 290.64(8)$ Å^3, $Z = 2$, $D_{calcd} = 6.116$ g cm^{-3}, $\mu = 57.817$ mm^{-1}, GOF = 1.111, $R_1 = 0.0324$, $\omega R_2 = 0.0722$ for data $I > 2\sigma(I)$, $R_1 = 0.0389$, $\omega R_2 = 0.0750$ for all data. Absolute structure parameter is 0.030(19). Data collections on an Agilent Technologies Super Nova Dual Wavelength CCD diffractometer equipped with a graphite-monochromated Mo-K_α radiation ($\lambda = 0.71073$ Å) at 293 K. Absorption corrected by Multi-scan method, structures solved by the direct methods (SHELX-97) and refined by full matrix least-squares method (SHELX-97). ICSD reference no. 428943. (See SI for details.). Further details on the crystal structure investigation may be obtained from the Fachinformationszentrum Karlsruhe, 76344 Eggenstein-Leopoldshafen, Germany (fax: (+49) 7247-808-666; e-mail: crysdata@fiz-karlsruhe.de), on quoting the depository number CSD-428943.
[21] Z.-T. Yu, Z. Shi, Y.-S. Jiang, H.-M. Yuan, J.-S. Chen, *Chem. Mater.* **2002**, *14*, 1314 – 1318.
[22] L.-Z. Wu, L. Cheng, J.-N. Shen, G.-Y. Yang, *CrystEngComm* **2013**, *15*, 4483 – 4488.
[23] H.-R. Tian, W.-H. Wang, Y.-E. Gao, T.-T. Deng, J.-Y. Wang, Y.-L. Feng, J.-W. Cheng, *Inorg. Chem.* **2013**, *52*, 6242 – 6244.
[24] a) H. Y. Li, H. P. Wu, X. Su, H. W. Yu, S. L. Pan, Z. H. Yang, Y. Lu, J. Han, K. R. Poeppelmeier, *J. Mater. Chem. C* **2014**, *2*, 1704 – 1710; b) H. W. Yu, S. L. Pan, H. P. Wu, W. W. Zhao, F. F. Zhang, H. Y. Liab, Z. H. Yang, *J. Mater. Chem.* **2012**, *22*, 2105 – 2110.
[25] L. Y. Li, G. B. Li, Y. X. Wang, F. H. Liao, J. H. Lin, *Chem. Mater.* **2005**, *17*, 4174 – 4180.
[26] L. X. Chang, L. Wang, X. Su, S. L. Pang, R. Hailili, H. W. Yu, Z. H. Yang, *Inorg. Chem.* **2014**, *53*, 3320 – 3325.

